Fabrication of Gold Nano-Particle Based Sensors Using Microspotting and DEP Technologies

Siu Ling Leung[1], Minglin Li[2], Fong Ting Lau[1], and Wen J. Li[1,2*]

[1]Centre for Micro and Nano Systems, The Chinese University of Hong Kong, Hong Kong, China
[2]State Key Lab of Robotics, Shenyang Institute of Automation, CAS, Shenyang, China
([*]E-mail: wen@mae.cuhk.edu.hk)

Abstract: We have shown that Au nanoparticles (Au NPs) pearl chain could be formed consistently between microelectrodes by combining microspotting and DEP technologies. Experimental results on varying the Au particle size and dielectrophoretic (DEP) parameters, including voltage and frequency, are reported in this paper to explore the critical parameters in controlling the Pearl Chain Formation (PCF) process between microelectrodes. PCF was observed from 10kHz to 5MHz for 100nm Au NPs, and 100kHz to 10MHz for 10nm Au NPs. Variations in formation rate were detected when the applied voltage and particle size varied. With higher voltage, pearl chain began to form at higher rate and the formation time decreased. The optimum frequency of the Au NPs PCF shifted to higher frequency region when the particle size decreased. Theoretical analysis was carried out by applying the theories of DEP force and AC electrokinetics to explain the observations with the DEP frequency ranging from 10 Hz to 10MHz. Finally, Au nanoparticle chains formed between the microelectrodes were shown to vary in resistance when environmental temperature was changed, indicating that these Au particle sensors could potentially be used to sense temperature and other thermal-based physical phenomena.

Keywords: AC electrokinetics, Dielectrophoresis Force, Gold Collodial Particles, Micro-spotting

1. INTRODUCTION

Gold Nanoparticles (NPs) or colloidal have been extensively studied because of their potential applications in nano-medicine [1-2], nano-photonics [3] and nano-devices [4]. In the past few decades, varieties of nanowire fabrication techniques were developed. One common methodology of nanowire growth is vapor-liquid-solid (VLS) synthesis method first reported in 1964 by Wanger and Ellis [5]. Semiconductor nanowires is fabricated via using gold nanoparticles as catalysts. Recently, dielectrophoretic (DEP) technique is used to manipulate gold nanoparticles directly (e.g., see [2,6]).

DEP technique assembles nanowires in a single step [7], in which dielectric particles experience a force enhanced by a non-uniform electric field as a result of polarization. However, during DEP manipulation, a large power density is generated in the fluid surrounding the electrodes when a high electric field is applied to manipulate small particles [9]. In order to achieve the optimum formation rate of gold pearl chain, both theoretical and experimental studies are presented in this paper. Moreover, to minimize the production time and cost, we have combined the DEP gold pearl chain batch manipulation and micro-spotting technology. As a result, gold NP-based sensors can be precisely and effectively fabricated.

2. THEORY

2.1 DEP Nanoparticles(NPs) Manipulation

Dielectrophoresis (DEP) is defined as the lateral motion generated on uncharged particles due to polarization induced by non-uniform electric fields [7]. The dielectrophoresis force exerted on NPs can be written as:

$$< F_{DEP}(t) >= 2\pi\varepsilon_m a^3 \,\mathrm{Re}[K(\omega)]\nabla \mid E_{rms} \mid^2 \qquad (1)$$

whereω is the angular frequency, E_{rms} is the root-mean-square (RMS) of electric field intensity, ε_m is the dielectric permittivity of the medium, a is the radius of the particles, and K is the Clausius-Mossoti factor which is given by:

$$K(\omega) = \frac{\varepsilon_p^* - \varepsilon_m^*}{\varepsilon_p^* - 2\varepsilon_m^*} \qquad (2)$$

Where ε_p^* and $\varepsilon_m^*$are the complex permittivity of the particle and the medium, respectively. The complex permittivity is given by:

$$\varepsilon^* = \varepsilon - j\frac{\sigma}{\omega} \qquad (3)$$

where σ is the conductivities of the medium [9].

The magnitude and direction of dielectrophoresis force are governed by the magnitudes of the applied electric field intensity, freqency, phyisical dimensions of NPs, and the real part of Clausius–Mossotti (CM) factor, respectively. The electric fieldintensity is determined by both the applied voltage and geometry of the electrodes. The former factor is proportional to the magnitude of DEP force and the latter factor determines the formation position of the NPs chains.

The frequency of the input AC signal govers the Clausius-Mossoti (CM) factor. The real part of CM factor determines the direction of the dielectrophoresis force and it varies form -0.5 to 1.0 for spherical particles.For positive CM factor, positive DEP force will be generated. NPs will move towards strong electric field region and draw downwards to the edges of the electrodes. The opposite situation occurs for negative DEP [2]. Fig.1 shows the real part of CM factor for single shell sperical particles. In our experiment, gold colloidal particles are coated with chemical stabilizer therefore particles are considered as a single shell model instead of a homogeneous dielectric sphere.

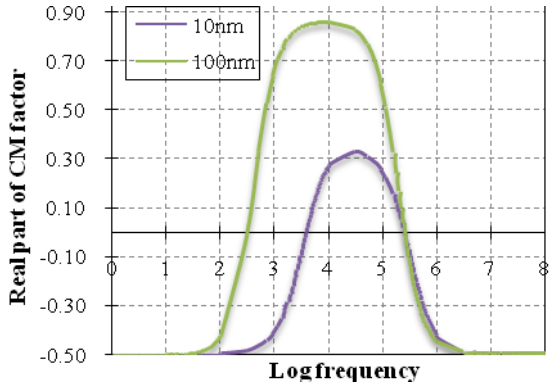

Fig. 1 The real part of CM factor for gold colloidal particles with 10nm and 100nm diameter suspended in D.I. water.

Under positive DEP force, NPs move towards strong electric field region. When a NP reaches the electrode, it will share the same potential as the electrode and thus the electric field intensity is modified to be higher at its free end. Other NPs in the bulk will move towards the free end (the high electric field region). Eventually, NPs chain will form across the electrode gap.

2.2Electric induced fluid flow

In our experiment of NPs manipulation, NPs are dispersed inside a liquid medium. Fluid flow, which is induced by electrothermal body force and AC electroomosis, is imparted on the manipulation process. Electrothermal force is induced because of a high power density is generated in the fluid surrounding the microelectrode when a high electric field is used to manipulate small particles [8]. The electrothermal body force on the fluid can be written as

$$< f_e >= \frac{2}{\pi^3 k} \frac{\sigma V_{rms}^4}{r^2} \prod (1 - \frac{2\theta}{\pi}) \hat{\theta} \quad (4)$$

where

$$\prod = \left[\frac{\alpha - \beta}{1 + (\omega \tau_q)^2} - \frac{\alpha}{2} \right] \quad (5)$$

where V_{rms} is the RMS of applied potential, k is thermal conductivity of the medium, $\alpha=(1/\varepsilon)(\partial\varepsilon/\partial T)$, $\beta=(1/\sigma)(\partial\sigma/\partial T)$ and τ_q is the charge relaxation time (ε/σ). An order of magnitude for a typical fluid flow velocity can be calculated by:

$$|u| = |f_e| \frac{l_o^2}{\eta} \quad (9)$$

Where l_o is the characteristic distance of microelectrode [9].

A simulation of the order of magnitude of the maximum fluid flow velocity(θ equal to 0 or π)under different medium conductivities is shown in Table 1. The magnitude of the induced fluid flow velocity is proportional to the medium conductivities. The applied field frequency determines the direction of the flow. When the frequency of applied signal is smaller than relaxation frequency, fluid flows away from the inter-electrode gap and compete with the DEP manipulation. The opposite situation occurs when the applied signal is higher than the relaxation frequency.

Table 1 Calculation on the Order of magnitude of the maximum fluid flow velocity generated by electrothermal body force for gold nanoparticles suspended in water

Solvent Conductivity (Sm^{-1})	Charge Relaxation frequency τ_q (s^{-1})	Order of magnitude of the fluid flow velocity generated by electrothermal body force (Note: "-" indicates movement away from electrodes)	
		Frequency $< \tau_q$	*Frequency* $> \tau_q$
5.5×10^{-6}	7.76×10^{3}	-10^{-5}	10^{-6}
5.0×10^{-5}	7.06×10^{4}	-10^{-4}	10^{-5}
5.0×10^{-4}	7.06×10^{5}	-10^{-3}	10^{-4}
5.0×10^{-3}	7.06×10^{6}	-10^{-2}	10^{-3}
5.0×10^{-2}	7.06×10^{7}	-10^{-1}	10^{-2}

(Assumed V_{rms}= 8.487,ε_m=80ε, l_o=2μm and η=0.00089 Pa•s. For water, α= -0.4% per degree and β=+2% per degree.)

Despite the fluid flow generated by electrothermal force, fluid flow is also induced by AC electroomosis effect in low field frequency range. This happens since the charges in a layer between the surface and the electrolyte, called the double layer, experience a force when an electric field is applied tangential to a surface bathed in the electrolyte. Consequently, the movement of double layer charges pulls the fluid along the surface and generates a flow which opposite the DEP manipulation [9]. The fluid flow velocity strongly depends on both the frequency of applied electric field and the conductivity of solution.

Double layer not only generated the AC electroomosis effect, but also decreased the magnitude of DEP force. Double layer induced by electrostatic potential attracts

ions of opposite charge from solution and repels ions with like charge. A thin layer near the electrode surface is densely packed with counter ions and loosely packed with co-ions. Eventually, the applied potential drops across the double layer and the actual potential passes through the electrolyte decreases. Thus, the magnitude of DEP force for manipulating the NPs decreases. The dropping ratio is strongly dependent on the frequency of applied field and conductivities of medium [9,12].

3. EXPERIMENTAL SETUP

3.1 Micro-spotting system

A computer-controlled micro-spotting system was previously developed by our group [10]. Controlled volumes of solutions canbe precisely spotted across the microelectrodes, resulting in a high yield and high precision rapid assembly method for gold nanoparticle based sensors. The micro-spotting system, as shown in Fig.2, is integrated by: a computer controllable X-Y-Z micromanipulator (MP285, Shutter Instrument Company), a computer controllable hydraulic pump (V6 syringe drive modules, Kloehn Limited) and a CCD video camera connected to the microscope.A real-time microscopic image was observed on a computer screen and served as a visual aid for locating the capillary probe tips to the desired position.

During the experiment, acapillary probe with inner diameter of 50 µm and outer diameter of 150 µm was mounted on the X-Y-Z micromanipulator. After the substrate with the microelectrodes was placed onto the stage, the X-Y-Z micromanipulator moved theprobe to an appropriate position. A syringe pump connected to the probe was then injected the solution droplet to the substrate.A typical single droplet contact injection process was used in our experiment. Initially, the probe tip was moved to 30µm above the substrate. A pressure was applied to the probe through the syringe pump,and then a concave shaped solution was formed at the probe tip due to the surface tension and the droplet size was kept increasing. Once the solution touched the substrate, it was in contact with both the probe tip and substrate. The probe-solution-substrate connection was stable if the probe tip remainedstationary and no external force was applied. When the probe was moved upwards, the connection was broken and a droplet of solution was dropped onto the substrate.

To perform micro-spotting on a substrate with microelectrodes, we can input the positions of the microelectrodes manually or automatically by loading the CIF-mask file into the control program of the system. After aligning the initial position of the microelectrodes, the probe tip can be moved sequentially to positions above each microelectrode and spotted on them.

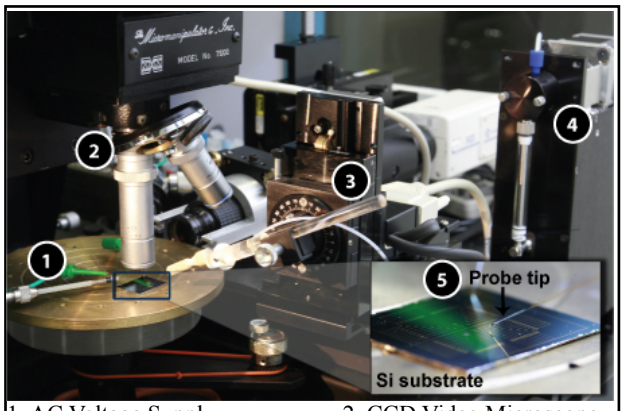

1. AC Voltage Supply 2. CCD Video Microscope
3. Micromanipulator 4. Syringe Pump
5. Probe

Fig.2 The micro-spotting system with CCD video, micromanipulator and syringe pump.

3.1 Experimental Detail

Au electrodes with gap separation of 2 µm (Fig. 3) were fabricated on Si/SiO2 substrates by a lift-off process. Si wafers were first cleaned by immersing then in acetone, followed by IPA, and finally in DI-water. Then photoresist (AZ5214E) was spin-coated on the wafers at 3000rpm. The photoresist was then patterned by negative lithography. Finally, layers of 500Å chromium and 3000Å gold films were deposited on top of the patterned photoresist by thermal evaporation before lift-off.

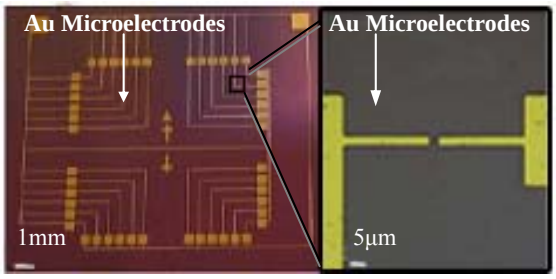

(a) (b)

Fig. 3 (a) Micro-photograph of Au microelectrodes fabricated on aSi substrate.(b) Optical image showing a pair of microelectrodes.

Controlled volume of gold colloidal solution (EM. GC series from British Biocell International, Cardiff, U.K.) with a diameter of 10 nm and 100 nm particles were precisely spotted across the microelectrodes by single droplet contact injection method using the micro-spotting system. The Au microelectrodes were excited by an AC voltage of typically $14V_{pk\text{-}pk}$ with a frequency 50kHz for 100nm Au NPs or 100kHz for 10nm Au NPs. DEP force was induced across the microelectrodes and the gold pearl chain was formed. Fig. 4 shows the SEM images of the gold peral chain formed by 10nm Au NPs and 100nm Au NPs. The gold microelectrodes were connected to 3kΩ resistorsin series to prevent overheat and undesired growth of the nanowires [12].

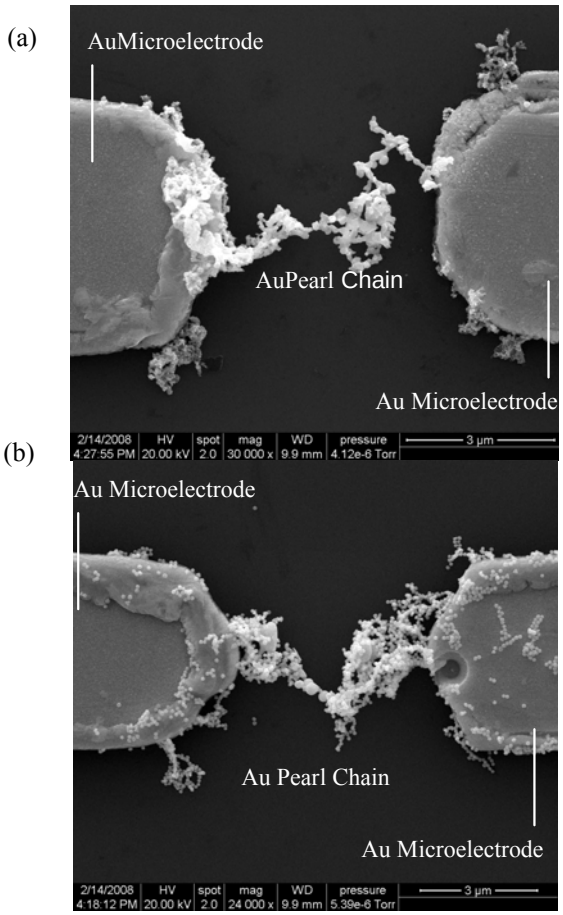

Fig. 4 SEM images of the gold pearl chain formed with (a) 10nm Au NPs and (b) 100 Au NPs.

4. RESULTS AND DISCUSSIONS

4.1Exploring the optimum frequencies

The direction of the dielectrophoresis force is determined by the real part of CM factor, which is governed by the applied frequency. Fig.5 shows a comparsion of the experimental result of PCF with the theordical calculated CM factor among varies frequency. It shows that pearl chain can be sucessfully formed across the microelectrodes when the CM factor is positive. Besides the direction of DEP force, the applied frequency also determined the direction and magnitude of fluid flow. Under low frequency range, both AC electroomosis and electrothermal body force induce fluid flow which move away from the electrode and working against the peral chain formation (PCF) manipulated by DEP force.The maxium fluid velocity induced by AC electroomosis is in the order of 10^{-2} whereas the particle velocity induced by DEP force is in the order of 10^{-4} and 10^{-2} for 10nm and 100nm Au NPs respectively. In our experiment, the magnitude of fluid velocity induced by AC electroomosis is reached maximum when applied frequency was equal to 10 Hz and minimize to zero when applied frequecy was higher than 100Hz. Previously, our group have investigated that the conductivity of the colloidal solution is ~5.0 × $10^{-5}Sm^{-1}$[12]. Refering to Table 1, the fluid velocity induced by electrothermal force is in the order of 10^{-4} for applied frequency lower than 70.6kHz. When applied frequency is higher than 70.6kHz, the fluid velocity is in the order of 10^{-5}in a direction moving towards the microelectrode.The particle manipulation by DEP force is enhanced by the fluid flow.Experimental result on pearl chain formation is shown in Fig. 6. The optimum frequency for 100nm and 10nm Au NPs is 50kHz and 100kHz respectively.

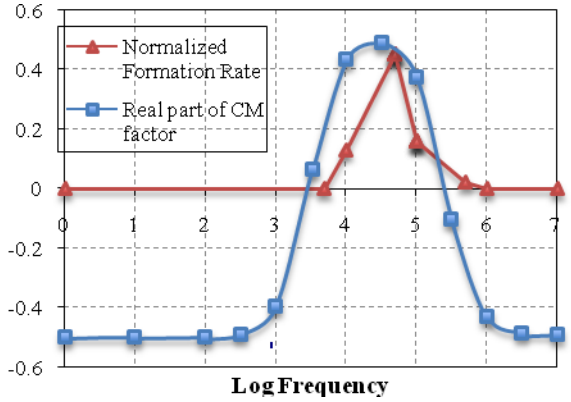

Fig. 5 Comparsion of the experimental PCF of 100nm under $12V_{pk-pk}$ applied voltage as a function of frequency with the theoretical calculation of CM factor for 100nm single shell model sphere.

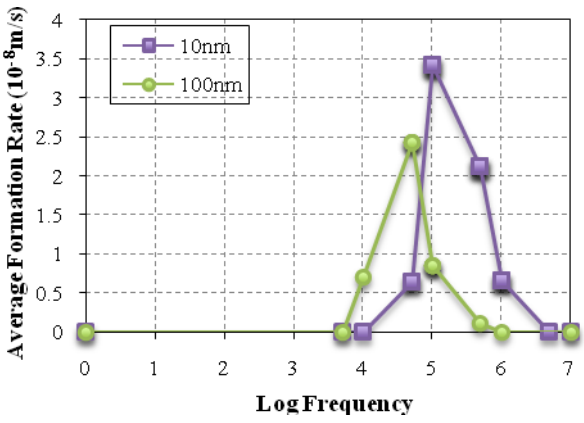

Fig. 6 Average PCF rates of Au NPs under $12V_{pk-pk}$applied voltages

4.2 Exploring the optimum voltages

According to the DEP equation (1), the magnitude of DEP force increases with voltage,a high voltage should be applied to the circuit in order to maximize the formation rate of the gold pearl chain. However, within the optimum frequency range, the electrothermal force induced fluid flow around the electrode. Comparing the DEP force equation (1) with the electrothermal body force equation (4), the magnitude of DEP force is proportional to V^2 whereas the electrothermal force is proportional to V^4. When the applied voltage increases, the increase of the electrothermal fluid velocity is larger than the increase of particle velocity driven by the DEP force.The influence of fluid flow becomes more significantunderhigh-applied voltage and the formation

rate of the gold pearl chainslowed down. Fig. 7 estimates the ratio of particle velocity to fluid velocityfor 10nm Au NPs under varies applied voltage, where

$$\gamma = \frac{particle \quad velocity \quad (v_{DEP})}{fluid \quad velocity \quad (v_{Electrothermal})} \quad (10)$$

The ratio change from 97.7 to 3.44 when applied voltages varies from $1V_{pk\text{-}pk}$ to $27V_{pk\text{-}pk}$.

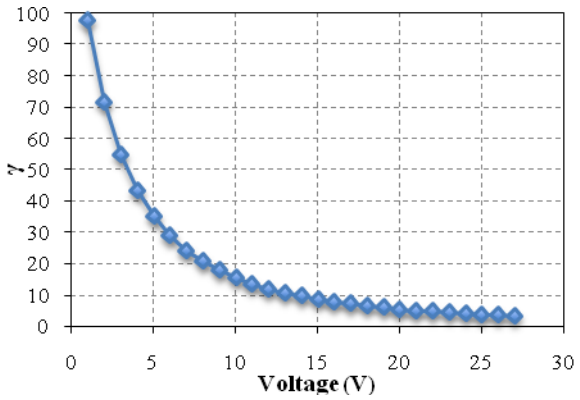

Fig. 7 Comparison between the particle velocity generated by DEP force and the fluid velocity generated by electrothermal body force for 10nm Au NPs in 100kHz frequency.

In 100nm Au NPs case, the particle velocity generated by DEP force is in the order of 10^{-2}. When applied voltage ranges from $3V_{pk\text{-}pk}$ to $18V_{pk\text{-}pk}$, the particle velocity is at least a hundred times higher than the fluid flow velocity. Experimental results in PCF rate under varies applied voltage is shown in Fig. 8. In conclusion, the influence of electrothermal force minimize when the particle size increase and the formation rate isproportional to V^2. Although high voltage can manipulate a high formation rate, the microelectrodes would melt because of the high temperature caused by the high voltage. From experimental observations, the best voltage for formation is range from $12V_{pk\text{-}pk}$ to $16V_{pk\text{-}pk}$ in order to maintain high formation rate and prevent melting of microelectrodes.

4.3 Influence of particle size to the formation rate

Dielectrophoresis force equation (1) shows that the magnitude of DEP force increases with the particle radius. However, in Fig. 6, the formation rate of 10nm Au NPs is similar to that of 100nm Au NPs. Moreover, the optimum frequency of the gold NPs PCF shifts to higher frequency region when the particle size decreases.Due to the influence of electrothermal fluid flow, difference between the experimental result and the theoretical calculation in formation rate induced by DEP force is obtained. From Table 1, when applied frequency is lower than 70.6kHz, fluid flows away from the microelectrode and works against the pearl chain formation. However, when the applied frequency is higher than the charge relaxation frequency, fluid flows towards the electrode and enhances PCF. In 10nm case, the optimum frequency for formation is 100kHz, which is higher than the charge relaxation frequency (~70.6 kHz). PCF is enhanced by electrothermal fluid flow. Whereas the optimum frequency is 50kHz for 100nm case, opposite situation occurred.The formation rate is slower due to the influence of fluid flow.

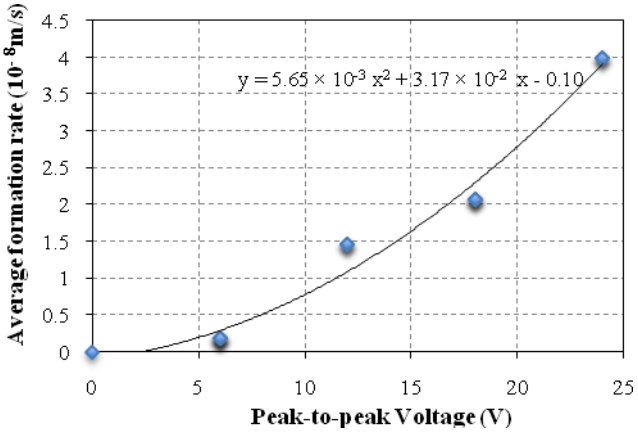

Fig. 8Average formation rates for 100nm Au NPs under varies voltages with frequency 50kHz

4.4 I-V Characteristics

I-V Characteristics of the gold nanoparticle based sensor was determined by a source meter (Model 2400 General-Purpose Source Meter, Keithley, Instruments, Inc.), which shows that the sensor could be operated in ~mW. The measured resistance of the sensor was ~100Ω. Variation of resistance between different sensors was found because of the random connections between nanoparticles during the DEP manipulation process. In spite of the variations, all samples were found of similar linear I-V characteristics, which obeyed the Ohm's Law.

4.5 Thermal Sensitivity

The sensor chip, packaged on a printable circuit board (PCB), was put inside a programmable climate chamber (KBF-115, Binder Co., Germany). The resistance change of the Au NP-based sensor was measured against the temperature inside the chamber. A few thermal annealing cycles from 20°C to 80°C for 5 cycles were performed. A representative and repeatable data set is shown in Fig. 9. A considerably room temperature resistance drift is observed due to the detachment of some gold nanoparticles.

The TCR determined the thermal sensitivityof the Au NP-based sensors. An increase in resistance is measured when the temperature increase, which implied the thermal sensing capability of the sensor. The TCR was obtained by measuring the resistance change of the gold nanoparticles based sensor with corresponding temperature and was calculated by

$$R(T) = R_o(1 + \alpha(T - T_o)) \quad (11)$$

where R_o is the resistance at room temperature T_o, and α is the temperature coefficient of resistance. The TCR of the sensor was found to be around 0.1%/°C.

The thermal response implies that the sensor is potentially applied to sense other thermal based physical phenomena, for example airflow sensing.A preliminary airflow sensing experiment was conducted under room temperature. Compressed air with difference pressure was introduced onto the sensor and the resistance change was measured. The experiment results in Fig. 10 shows that the measured resistance dropped when airflowwas passed through andit raised back when the airflow was stopped. This happens due to the heat loss induced by the airflow. Thechange of resistanceincrease with the pressure of the input airflow, the average resistance change under varies pressure is plotted in the inset of Fig. 10.

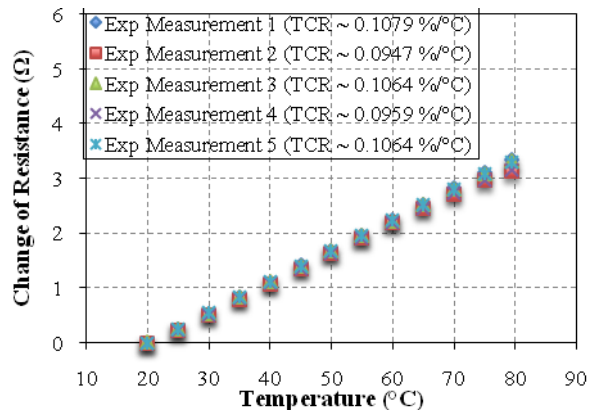

Fig. 9 TCR variation of the gold NP-based sensor in five consecutive measurements.

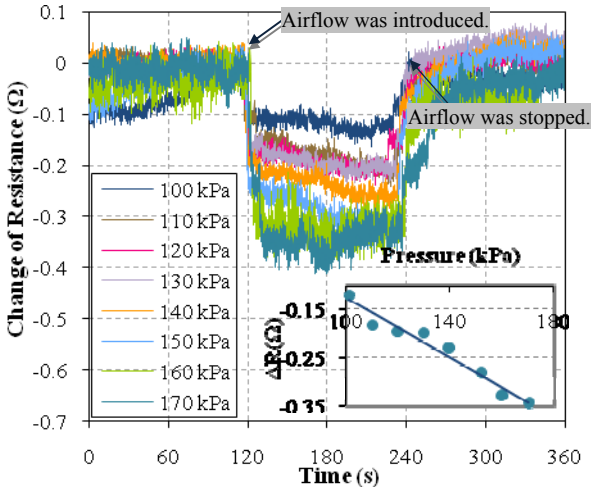

Fig. 10 Electrical responses of the gold NP-based sensor against airflow with vary pressure. (Inset) Resistance-pressure dependency of the sensor.

CONCLUSION

Fabrication of gold nanoparticle based sensor by combining the micro-spotting and DEP technologies was presented. With the micro-spotting system, gold pearl chain can be rapidly and precisely formed across microelectrode with a low production cost. Through the theoretical study and experimental observation of particle manipulation by DEP force and AC electrokinetic fluid flow, critical condition for PCF was investigated. The optimum frequency for manipulating 10nm and 100nm Au NPs are 50kHz and 100kHz respectively, and the optimum voltage is in the range of $12V_{pk\text{-}pk}$ to $16V_{pk\text{-}pk}$. The I-V characteristics and TCR of the sensor was performed on several samples. The temperature-resistance response indicates that these Au particle sensors could potentially be used as a low powerthermal sensor, for example, airflow sensor.

ACKNOWLEDMENT

The authors acknowledge all the members at the Centre for Micro and Nano Systems (CMNS) for their support and encouragement. In particular, the authors would like to thank Dr. W. Y. Cheung, Dr. Yan Li Qu, Ms. Winnie W. Y. Chow, Ms. Heidi Y.Y. Wong and Mr. Ho Shing Poon for their help on this project and the useful discussions.

REFERENCES

[1] R. G. Grainger, "Intravascular Contrast Media—the Past, the Present, and the Future," *Br. J. Radiol.*,vol. 55, no. 1, 1982.

[2] L. F. Zheng, S. D. Li, and P. J. Burke, "Self-Assembled Gold Nanowire from Nanoparticles: An Electronic Route Towards DNA Nanosensors," *Nanoengineering: Fabrication, Properties, Optics and Devices,* SPIE vol. 5515, 2004.

[3] G. W. Leung, F. T. Lau, S. L. Leung, and W. J. Li, "Formation of Au Colloidal Crystals for Optical Sensing by DEP-Based Nano-Assembly,"*The 2nd IEEE Conference on Nano/Micro Engineered and Molecular Systems,* January 16, 2007.

[4] S. I. Khondaker, "Fabrication of Nanoscale Device Using Individual Colloidal Gold Nanoparticles," *IEE Proc-Circuits Devices Syst*.,vol. 151, no.5, 2004.

[5] R. S. Wagner and W. C. Ellis, "Vapor-Liquid-Solid Mechanism of Single Crystal Growth," *Applied Physics Letters,* Vol.4, No.5, 1964.

[6] R. Kretschmer and W. Fritzsche, "Pearl chain formation of nanoparticles in microelectrode gaps by dielectrophoresis," *Langmuir*, Vol. 20, No. 26, pp. 11797-801, 2004

[7] H. A. Pohl, "Dielectrophoresis," *Cambridge University Press,* 1978.

[8] A. Ramos, H. Morgan, N. G. Green and A. Castellanos, "AC Electrokinetics: a review of*: Appl. Phys 31, 1998.*

[9] H. Morgan and N. G. Green, "AC Electrokinetics colloidal and nanoparticles," *Research Studies Press Ltd., 2003.*

[10] W. C. Lai, K. M. Fung, and W. J. Li, "A Systematic Approach to Fabricate CNT-Based Nano Devices: Combining DEP and Microspotting Techologies," *The 5th IEEE International Conference on Nanotechnology,* July 11, 2005.

[11] M. L. Li, F. Fei, Y. L. Qu, Z. L. Dong, W. J. Li, and Y. C. Wang, "Theoretical Analysis Based on Particle Electro-Mechanics for Au Pearl Chain Formation," *The 7th IEEE International Conference on Nanotechnology*, August 03, 2007.

[12] S. L. Leung, M. L. Li, and W. J. Li, "Formation of Gold Nano-particle Chains by DEP – a Parametric Experimental Analysis," *The 3rd IEEE International Conference of Nano/Micro Engineered and Molecular Systems*, January 9, 2008.